HHS Public Access

Author manuscript

Neurobiol Aging. Author manuscript; available in PMC 2021 March 01.

Published in final edited form as:

Neurobiol Aging. 2020 March ; 87: 78–88. doi:10.1016/j.neurobiolaging.2019.11.011.

Medial Temporal Lobe White Matter Pathway Variability is Associated with Individual Differences in Episodic Memory in Cognitively Normal Older Adults

Kylie H. Alm[1], **Andreia V. Faria**[2], **Abhay Moghekar**[3], **Corinne Pettigrew**[3], **Anja Soldan**[3], **Susumu Mori**[2], **Marilyn Albert**[3], **Arnold Bakker**[1]

[1]Department of Psychiatry and Behavioral Sciences, Johns Hopkins University School of Medicine

[2]Department of Radiology, Johns Hopkins University School of Medicine

[3]Department of Neurology, Johns Hopkins University School of Medicine

Abstract

Significant evidence demonstrates that aging is associated with variability in cognitive performance, even among individuals who are cognitively normal. In this study, we examined measures from magnetic resonance imaging (MRI) and cerebrospinal fluid (CSF) to investigate which measures, alone or in combination, were associated with individual differences in episodic memory performance. Using hierarchical linear regressions, we compared the ability of diffusion tensor imaging (DTI) metrics, CSF measures of amyloid and tau, and gray matter volumes to explain variability in memory performance in a cohort of cognitively normal older adults. Measures of DTI microstructure were significantly associated with variance in memory performance, even after accounting for the contribution of the CSF and MRI gray matter volume measures. Significant associations were found between DTI measures of the hippocampal cingulum and fornix with individual differences in memory. No such relationships were found between memory performance and CSF markers or gray matter volumes. These findings suggest that DTI metrics may be useful in identifying changes associated with aging or age-related diseases.

Keywords

cognitive aging; biomarker; diffusion tensor imaging; cerebrospinal fluid; episodic memory

Correspondence concerning this article should be addressed to Arnold Bakker, Johns Hopkins University School of Medicine, 600 North Wolfe Street, Baltimore, MD 21287, abakker@jhu.edu.

Disclosure statement

AM receives funding from Fujirebio Diagnostics Ltd. (no direct payments, salary support, or consultation fees). SM is part owner and CEO of “AnatomyWorks”. This arrangement is being managed by the Johns Hopkins University in accordance with its conflict of interest policies. The remaining authors declare no competing interests.

1. Introduction

Alzheimer's disease (AD) is the most common form of dementia and the sixth-leading cause of death in the United States (Alzheimer's Association, 2017). Mounting evidence suggests that neuropathological changes associated with AD may be present up to decades before any clinical symptoms arise (Sperling et al., 2011). Recent research has therefore focused on examining cognitively normal individuals across a range of ages in an effort to identify subtle alterations in cognition, and related biomarkers, that may precede clinical symptom onset of AD. In one such study, the Biomarkers of Cognitive Decline Among Normal Individuals (BIOCARD) study (Albert et al., 2014), cognitively normal individuals were enrolled primarily during middle-age and followed longitudinally for over 20 years. Assessments included a comprehensive clinical and cognitive evaluation, as well magnetic resonance imaging (MRI) and cerebrospinal fluid (CSF) collection. The present study utilized cross-sectional data from this cohort to examine the relationship of MRI and CSF measures to episodic memory performance in cognitively normal middle aged and older individuals.

A large number of studies have examined volumetric MRI changes associated with aging and the early phases of AD (e.g. Miller et al., 2015a, 2015b, 2013; Soldan et al., 2015). Recently, more attention has been drawn to alterations in white matter fiber bundles, the structural pathways that connect disparate neural regions throughout the brain, and changes associated with aging and early AD (for reviews, see Bennett and Madden, 2014; Caso et al., 2016; Contreras et al., 2015; Oishi et al., 2011; Radanovic et al., 2013). Diffusion tensor imaging (DTI) is a well-suited technique for such investigations, since DTI methodologies allow for the quantification of white matter microstructure, which may enable better detection of subtle variations that may be present even among cognitively normal individuals, compared to changes on the macrostructural level. In fact, microstructural aberrations have been demonstrated in cognitively normal older adults, as well as patients with mild cognitive impairment (MCI; Amlien and Fjell, 2014; Clerx et al., 2012; Gold et al., 2012; Lam et al., 2017; Nobili et al., 2014; Teipel et al., 2016; Zhang et al., 2014), and suggest a spatiotemporal pattern to the microstructural changes, with the earliest alterations beginning in limbic tracts, followed by more lateral temporoparietal association tracts, and ultimately progressing to long-range frontal pathways (Teipel et al., 2016). Teipel and colleagues (2016) also noted that the early limbic tract alterations tend to be the most severe and can be detected years before gray matter atrophy or cognitive impairment is observed.

Microstructural variation in limbic white matter pathways has also been consistently associated with episodic memory function, which is typically the earliest cognitive manifestation of AD. The fornix, for example, which connects the hippocampus to the mammillary bodies, is known to play a critical role in facilitating episodic memory processing, and its microstructure has been related to variability in memory performance in both cognitively normal older adults and patients with MCI. Specifically, fornix microstructure was associated with performance on tests of verbal free recall in cognitively normal participants (Metzler-Baddeley et al., 2011a), as well as MCI patients (Mielke et al., 2012; Oishi et al., 2012), and further associated with visual recall performance in cognitively normal participants (Metzler-Baddeley et al., 2011a). Similarly, the hippocampal cingulum,

which connects the hippocampus and parahippocampus to the inferior parietal lobe, has been associated with verbal recall performance in non-demented older adults (Ezzati et al., 2016; Metzler-Baddeley et al., 2011a), and both verbal and visual recall in MCI patients (Lin et al., 2014). Finally, associations have been found with the uncinate fasciculus (UF), which connects the anterior and medial temporal lobes (MTLs; including portions of the entorhinal cortex, parahippocampal cortex, and perirhinal cortex) to the orbitofrontal cortex (OFC). Although fewer studies have examined these relationships in cognitively normal older adults, reports have demonstrated that UF microstructure is related to performance on a paired associates task among cognitively normal participants (Metzler-Baddeley et al., 2011a), while in MCI patients, the relationship has been demonstrated with verbal recall (Hiyoshi-Taniguchi et al., 2015). Taken together, these findings suggest that the microstructural properties of these three pathways may be particularly relevant in the context of age- and disease-related changes in cognition.

CSF measures are well-established as biomarkers of AD. They have been used as proxies for quantification of the two hallmark neuropathological features of AD: amyloid plaques and neurofibrillary tangles (Braak and Braak, 1991; Thal et al., 2002). CSF $Aß_{42}$ is used to index amyloid-beta (Aß) protein deposition, while CSF total tau (t-tau) and phosphorylated tau (p-tau) are measures associated with neurodegeneration and the pathological build-up of tau proteins within neurofibrillary tangles, respectively (Fagan et al., 2007; Gustafson et al., 2007). Recent evidence indicates that CSF AD biomarkers predict longitudinal cognitive decline among cognitively normal individuals (Soldan et al., 2016; Vos et al., 2013), as well as progression to MCI (Moghekar et al., 2013). Evidence remains mixed, however, as to whether cross-sectional measures of CSF and cognitive performance are related in cognitively normal participants. A few studies have detected cross-sectional correlations between CSF markers and episodic memory performance ($Aß_{42}$: Stomrud et al., 2010; t-tau and p-tau, but not $Aß_{42}$: Pettigrew et al., 2015). However, it has been more common for studies to report no evidence of a relationship with $Aß_{42}$ or tau markers (Li et al., 2014; Rami et al., 2011; Rolstad et al., 2011; Schott et al., 2010; Vemuri et al., 2011), at least for cognitively normal participants.

Although CSF markers may demonstrate weak associations with cross-sectional cognitive performance when examined in isolation, they may add meaningful information when examined in combination with other biomarkers, such as DTI metrics. However, research comparing the relative contributions of DTI and CSF measures to variability in cognition has been very limited (for a review, see Alm and Bakker, 2019). The present investigation, therefore, sought to explore the combined use of DTI and CSF metrics in explaining variance in episodic memory performance cross-sectionally. We aimed to test whether measures of DTI microstructure, CSF markers, gray matter volumes, white matter volumes, or a combination of these metrics were significantly related to delayed memory performance in cognitively normal participants in the BIOCARD cohort. Hierarchical regression analyses were used, so that each class of metrics could be added as independent variables within the overall model in a step-wise fashion. This allowed us to assess the relative contributions of each category of variables to the proportion of explained variance in episodic memory performance. Gray matter volumes were included in our models to ensure any potential DTI effects were present above and beyond the potential effects of gray matter volume. In a

separate analysis, we tested whether white matter volume of the structures of interest related to variability in delayed episodic memory.

2. Materials and Methods

2.1. Study design

Data included in the present investigation were obtained from a subsample of participants enrolled in the BIOCARD study, a longitudinal study designed to identify biomarkers of the earliest phases of AD. The BIOCARD study began in 1995 under the auspices of the intramural program of the Geriatric Psychiatry Branch of the National Institutes of Mental Health (NIMH). During this time, participants underwent annual assessments comprised of a comprehensive neuropsychological battery and clinical evaluation. Approximately every two years, MRI data, CSF samples, and blood specimens were collected. The study was stopped in 2005 for administrative reasons. In 2009, a research team at Johns Hopkins University (JHU) was funded to re-initiate the study. Participants again began to undergo annual cognitive and clinical assessments, and in 2015, biennial collection of MRI (including diffusion-weighted imaging) and CSF data was initiated, and amyloid PET data were acquired. The data presented here were collected beginning in 2015. Data collection is ongoing.

2.2. Participants

The overall BIOCARD study sample consists of 349 individuals who were recruited between 1995 and 2005. At the time of enrollment, participants were primarily middle-aged (M = 57.3, SD = 10.4, range = 20 – 85). Participants underwent a comprehensive evaluation comprised of a battery of neuropsychological tests, physical and neurological examinations, an electrocardiogram, and standard laboratory tests. At the time of enrollment, all participants were cognitively normal, as ascertained by cognitive testing, and free from any significant medical problems (e.g. severe cerebrovascular disease, epilepsy, or substance abuse). By design, approximately 75% of enrolled participants had a first degree relative with AD dementia. Additional information on the overall BIOCARD cohort is presented elsewhere (see Albert et al., 2014).

The current study sample consisted of 109 cognitively normal participants (60.6% female) who underwent MRI scanning, CSF collection, and cognitive testing between January 2015 and January 2017 as part of the ongoing longitudinal assessments of the larger BIOCARD cohort. The participants had a mean age of 69.22 (SD = 8.60, range = 34 – 89) and a mean of 17.52 years of education (SD = 2.09, range = 12–20). All of these participants were judged to be cognitively normal, based on the consensus diagnoses procedures completed by the staff of the JHU BIOCARD Clinical Core, which included neurologists, neuropsychologists, research nurses, and research assistants. All cases were handled in a manner comparable to those employed at the National Institute on Aging Alzheimer's Disease Centers program. First, a syndromic diagnosis was established (i.e., normal, MCI, Impaired Not MCI, Dementia). The syndromic diagnoses used three sources of information: (1) clinical data pertaining to the medical, neurological, and psychiatric status of the individual; (2) reports of changes in cognition by the individual and by collateral sources;

and (3) decline in cognitive performance, based on review of longitudinal testing from multiple domains (and comparison to published norms). Within the context of this study, the diagnosis of Impaired Not MCI typically reflected contrasting information from the CDR interview and the cognitive test scores (i.e., the subject or collateral source expressed concerns about cognitive changes in daily life, but the cognitive testing did not show changes, or vice versa, the test scores provided evidence for declines in cognition, but neither the subject nor the collateral source reported changes in daily life; see Albert et al., 2014 for details). Subjects with a diagnosis of Impaired Not MCI ($n = 20$) were therefore included among the group of cognitively normal participants. If a subject was not considered to be normal, then an etiologic diagnosis was made (e.g., AD, Frontotemporal Dementia, Lewy Body Dementia, etc.). These diagnostic procedures follow the guidelines of the National Institute on Aging – Alzheimer's Association working group (Albert et al., 2011; McKhann et al., 2011). All diagnoses were made without knowledge of the MRI or CSF biomarker measures.

2.3. Image acquisition and processing

MRI imaging was conducted on a 3T Philips Achieva scanner (Eindhoven, The Netherlands). Diffusion-weighted images were acquired from a spin echo sequence (TR = 7.5 s, TE = 75 ms, FOV = 260 × 260, slice thickness = 2.2 mm, flip angle = 90, b-value = 700, number of gradients = 33, axial plane). The image analysis was performed on an atlas-based matrix, which was generated by MRICloud (https://braingps.mricloud.org; Mori et al., 2016). DTI reconstruction and quality control were also performed using MRICloud, which follows the pipeline of DTIStudio (Jiang, Van Zijl, Kim, Pearlson, & Mori, 2006). MRICloud offers a fully automated multi-atlas image parcellation algorithm, which combines the image transformation algorithm, Large Deformation Diffeomorphic Metric Mapping (LDDMM; Christensen et al., 1997; Grenander and Miller, 1998; Miller et al., 1997) based on complementary contrasts (mean diffusivity (MD), fractional anisotropy (FA), and fiber orientation; Ceritoglu et al., 2009), and a likelihood fusion algorithm for DTI multi-atlas mapping and parcellation (Tang et al., 2014). The DTI multi-atlas template set contains 12 healthy adult brains, and results in the parcellation of 168 brain structures, from which vectors of DTI scalar metrics (three eigenvalues) and volumes were extracted.

We focused our analyses on MD, which is the average of the three eigenvalues, and radial diffusivity (RD), which is the average of the two minor eigenvalues, perpendicular to the major axis of diffusion. These diffusivity indices have been shown to be more sensitive to specific microstructural changes than FA, which is quite sensitive to general changes in microstructure, but is less likely to detect the particular type of change (Alexander et al., 2011). Although FA remains the most commonly reported measure, certain studies have shown that it is a suboptimal measure of underlying microstructure (e.g. Acosta-Cabronero et al., 2010; Leow et al., 2009). In addition, we sought to *a priori* restrict our number of comparisons in order to minimize inflated false positive rates due to multiple comparisons. Therefore, MD and RD were chosen as our specific microstructural measures of interest.

Five structures were defined for these analyses as *a priori* regions of interest (ROIs) based on their known involvement in episodic memory processes. DTI metrics of MD and RD, as well

as white matter volumes were used in our statistical analyses for the following ROIs: (1) the fornix (restricted to the body and column due to resolution constraints; see Supplementary Figure S1), (2) the hippocampal cingulum, and (3) the uncinate fasciculus (UF). The gray matter volumes of two ROIs were also included in the analyses: (1) the entorhinal area and (2) the hippocampus. ROI-specific MD and RD measures were obtained by averaging the MD or RD values across all of the voxels within an ROI. Volumes were measured by counting the number of voxels within an ROI. ROIs for each participant were visually inspected to ensure that the automated segmentation process yielded accurate delineations of the structures of interest.

2.4. CSF assessments

CSF specimens in the present study were collected beginning in 2015, when biospecimen collection was re-initiated at Johns Hopkins. CSF and MRI data were collected during the same visit. 20 ml CSF was collected in the morning between 8 and 10 am after an overnight fast into a 50 ml polypropylene tube. After mixing and centrifugation at 2000 rpm for 15 minutes, 500 ul aliquots of CSF were frozen at −80 °C within 60 minutes of collection. CSF $A\beta_{42}$ (picograms/ml) and CSF t-tau (picograms/ml) were measured using the Lumipulse G1200 assay (Fujirebio, Malvern, PA). Assays were run in duplicate, and all samples were run in a single batch. Intra-assay coefficient of variation for this assay was 3.1% for $A\beta_{42}$ and 4.3% for t-tau.

2.5. Delayed episodic memory composite score

A delayed verbal episodic memory composite score was derived from performance on tasks within the neuropsychological battery administered during the same visit as MRI data acquisition and lumbar punctures. Specifically, z-scored performance was calculated for the California Verbal Learning Test (CVLT) long delay free recall and the Wechsler Memory Scale Logical Memory (LM) delayed recall measures. For each participant, these z-scored measures were then averaged to yield a single delayed memory composite score.

2.6. Statistical analyses

Hierarchical linear regression analyses were used to examine the relationship between biomarker measures – including DTI metrics, CSF markers, and gray matter volume measures – and the composite measure of delayed episodic memory. The variabilities for each of the independent variables of interest are plotted in Supplementary Figure S2.

Separate models were constructed for each microstructural measure (i.e. MD and RD) in order to avoid multicollinearity. For all hierarchical regressions, the dependent measure was the composite delayed episodic memory score, and independent variables were added in a step-wise manner. Step 1 included independent variables corresponding to demographics, including age, sex, and years of education. In Step 2, DTI microstructural measures were entered as additional separate independent variables, including MD or RD of the hippocampal cingulum, fornix, and UF. To reduce the number of comparisons, microstructural measures were collapsed across hemispheres; however, it should be noted that comparable results were obtained when considering left and right hemispheres separately (data not shown). In Step 3, CSF measures of $A\beta_{42}$ and t-tau were entered as

additional separate independent variables. Finally, in Step 4, entorhinal and hippocampus volume measures (collapsed across hemispheres) were entered as additional separate independent variables. We included gray matter volume of the hippocampus and entorhinal area to determine whether associations with the white matter tracts were driven by volume differences in the gray matter regions where the pathways originate (Caso et al., 2016).

The same general procedure was followed to construct a hierarchical model to examine white matter volumes. The dependent measure remained composite delayed episodic memory score. The three demographic variables were entered in Step 1, followed by white matter volumes of the hippocampal cingulum, fornix, and UF (collapsed across hemispheres) in Step 2. Next, CSF $A\beta_{42}$ and t-tau were entered in Step 3, and gray matter volumes of the entorhinal area and hippocampus were entered in Step 4. Statistical analyses were performed using SPSS (version 24).

3. Results

3.1. Mean diffusivity explains variability in delayed episodic memory performance

First, a hierarchical regression model was constructed using mean MD of the MTL ROIs as the white matter measures of interest. Results are presented in Table 1. Step 1, including age, sex, and education was significant ($R^2 = 0.11$, $F(3, 105) = 4.27$, $p = .01$), with sex showing a significant association with delayed memory ($\beta = 0.26$, $t(105) = 2.79$, $p = .01$) such that female participants tended to perform better than males. Age and education did not reach significance (p's > .07).

In Step 2, the addition of mean MD measures resulted in a significant overall model ($R^2 = 0.17$, $F(6, 102) = 3.53$, $p = .003$), with a trend towards an enhanced proportion of variance explained by the model from the inclusion of these microstructural measures ($\Delta R^2 = 0.06$, $\Delta F(3, 102) = 2.60$, $p = .06$). Sex remained significant ($\beta = 0.28$, $t(102) = 3.05$, $p = .003$). Additionally, hippocampal cingulum MD and fornix MD both emerged as significant variables, each uniquely contributing to the proportion of explained variance ($\beta = 0.26$, $t(102) = 2.38$, $p = .02$ and $\beta = -0.29$, $t(102) = -2.18$, $p = .03$, respectively). Specifically, higher hippocampal cingulum MD and lower fornix MD were associated with better delayed memory performance. No other variables reached significance (p's > .56).

In Step 3, the addition of CSF $A\beta_{42}$ and t-tau yielded a significant overall model ($R^2 = 0.18$, $F(8, 100) = 2.74$, $p = .01$). However, adding these measures did not significantly increase the variance explained by the overall model ($\Delta R^2 = 0.01$, $\Delta F(2, 100) = 0.46$, $p = .63$). Sex ($\beta = 0.29$, $t(100) = 3.13$, $p = .002$), hippocampal cingulum MD ($\beta = 0.26$, $t(100) = 2.32$, $p = .02$), and fornix MD ($\beta = -0.31$, $t(100) = -2.29$, $p = .02$) remained significant in this step, but neither $A\beta_{42}$ or t-tau were significantly related to delayed memory performance ($\beta = -0.01$, $t(100) = -0.08$, $p = .93$ and $\beta = -0.09$, $t(100) = -0.89$, $p = .38$, respectively).

In Step 4, inclusion of the gray matter volumes yielded a significant overall model ($R^2 = 0.19$, $F(10, 98) = 2.33$, $p = .02$), but adding these variables did not change the amount of variance explained by the model ($\Delta R^2 = 0.01$, $\Delta F(2, 98) = 0.77$, $p = .47$). Therefore, the addition of gray matter volumes did not improve the model. Sex ($\beta = 0.27$, $t(98) = 2.47$, p

= .02), hippocampal cingulum MD ($ß$ = 0.25, $t(98)$ = 2.22 p = .03), and fornix MD ($ß$ = −0.34, $t(98)$ = −2.43, p = .02) all remained significant. No other variables reached significance (p's > .35). Partial regression plots for the significant associations derived from Step 4, which represent the unique relationship between the independent variable of interest and delayed memory performance after controlling for all other variables in the model, are depicted in Figure 1a. Partial regression plots for non-significant associations are presented in Supplementary Figure S3.

In order to ensure that this pattern of results was not dependent on the order in which the diffusion metrics were entered into the model, we also examined a hierarchical model where the MTL MD metrics were entered during Step 4, rather than Step 2. The results were consistent with the findings reported above. Only the addition of the MD metrics significantly increased the amount of variance explained by the model above and beyond the demographic variables (ΔR^2 = 0.07, $\Delta F(3, 98)$ = 2.84, p = .04). The full results of this model are presented in Supplementary Table S1.

3.2. Radial diffusivity explains variability in delayed episodic memory performance

For the next hierarchical model, mean RD values of the MTL structures served as the primary variables of interest. Results are presented in Table 2. For Step 1 (which included age, sex, and education as independent variables), the results were the same as described above. In Step 2, the inclusion of mean RD of the MTL structures yielded a significant overall model (R^2 = 0.19, $F(6, 102)$ = 4.03, p < .001), as well as a significant increase in the amount of explained variance accounted for by the model (ΔR^2 = 0.08, $\Delta F(3, 102)$ = 3.48, p = .02). The addition of microstructural RD indices significantly improved the model's ability to explain variability in memory performance. Female sex ($ß$ = 0.27, $t(102)$ = 2.99, p = .003), greater hippocampal cingulum RD ($ß$ = 0.31, $t(102)$ = 2.71, p = .01), and lower fornix RD ($ß$ = −0.37, $t(102)$ = −2.65, p = .01) were all significantly associated with better delayed memory performance. No other variables reached significance (p's > .54).

In Step 3, the overall model was significant (R^2 = 0.20, $F(8, 100)$ = 3.16, p = .003), but the amount of variance explained did not change significantly from Step 2 to Step 3 (ΔR^2 = 0.01, $\Delta F(2, 100)$ = 0.62, p = .54), indicating that adding measures of CSF $A\beta_{42}$ and t-tau did not improve the proportion of explained variance. In Step 3, sex, hippocampal cingulum RD, and fornix RD each remained significant (sex: $ß$ = 0.29, $t(100)$ = 3.10, p = .003; hippocampal cingulum RD: $ß$ = 0.31, $t(100)$ = 2.72, p = .01; fornix RD: $ß$ = −0.40, $t(100)$ = −2.80, p = .01). By contrast, neither $A\beta_{42}$ nor t-tau were found to be significantly related to delayed memory ($ß$ = −0.01, $t(100)$ = −0.11, p = .91 and $ß$ = −0.10, $t(100)$ = −1.03, p = .31, respectively). No other variables reached significance (p's > .53).

In Step 4, a similar pattern of results emerged. The overall model was significant (R^2 = 0.21, $F(10, 98)$ = 2.63, p = .01), but the inclusion of entorhinal and hippocampal volumes did not change the proportion of variance explained by the model (ΔR^2 = 0.01, $\Delta F(2, 98)$ = 0.61, p = .55). Once again, sex, hippocampal cingulum RD, and fornix RD remained significant, even after accounting for gray matter volumes (sex: $ß$ = 0.26, $t(98)$ = 2.43, p = .02; hippocampal cingulum RD: $ß$ = 0.30, $t(98)$ = 2.58, p = .01; fornix RD: $ß$ = −0.43, $t(98)$ = −2.88, p = .01). No other variables reached significance (p's > .29). The partial regression

plots from Step 4 for the fornix and hippocampal cingulum are depicted in Figure 1b. Partial regression plots for non-significant associations are presented in Supplementary Figure S3.

To confirm that these findings were not simply due to the order of variable entry into the hierarchical model, we also examined a model in which the DTI measures were entered last. Even when the MTL RD measures were entered in Step 4, this remained the only step where the proportion of explained variance increased significantly beyond the initial model with demographics only ($\Delta R^2 = 0.09$, $\Delta F(3, 98) = 3.70$, $p = .01$). The full hierarchical model is presented in Supplementary Table S2.

3.3. Examining potential partial volume effects

In order to account for potential confounds due to partial volume effects, we examined models in which both DTI microstructural measures and white matter volumes were included. This is especially a concern for smaller pathways, like the fornix, as structures with lower volumes tend to show higher partial volume effects (Vos et al., 2011). At Step 1, the regression model included the demographic variables. At Steps 2 and 3, DTI microstructural measures and white matter volumes corresponding to the structures of interest were included, respectively. With these variables in the model, the DTI microstructural relationships with delayed memory remained significant (hippocampal cingulum MD: $ß = 0.23$, $t(99) = 2.04$, $p = .05$; fornix MD: $ß = -0.34$, $t(99) = -2.52$, $p = .01$; hippocampal cingulum RD: $ß = 0.26$, $t(99) = 2.23$, $p = .03$; fornix RD: $ß = -0.40$, $t(99) = -2.83$, $p = .01$), suggesting that these associations were not merely the result of size differences in the white matter ROIs.

3.4. Examining the relationship of CSF ratios to variability in delayed episodic memory performance

Prior evidence suggests that the ratio of CSF tau to $Aß_{42}$ is a better predictor of clinical decline than each measure independently (Moghekar et al., 2013). Therefore, we also examined models in which this ratio was included. In this analysis, we used the ratio of t-tau/$Aß_{42}$ as an independent variable in the regression models, instead of separate variables for each measure. T-tau/$Aß_{42}$ was not significantly related to delayed memory in either model (MD model: $ß = -0.09$, $t(101) = -0.99$, $p = .32$; RD model: $ß = -0.10$, $t(101) = -1.05$, $p = .30$), nor did it change the overall pattern of results.

3.5. Examining the relationship of white matter volume to variability in delayed episodic memory performance

Finally, we tested whether the volume of the white matter ROIs explained variation in delayed memory composite scores. The general procedure for constructing the hierarchical model was the same, except that Step 2 was now comprised of white matter volume measures corresponding to the hippocampal cingulum, fornix, and UF. Results are presented in Table 3.

Given that Step 1 was the same as in the previous hierarchical models (i.e., demographic variables entered as separate independent variables, with delayed memory composite score as the dependent measure), the results are identical to those observed in Step 1 above.

In Step 2, the inclusion of white matter volumes yielded a significant overall model (R^2 = 0.16, $F(6, 102) = 3.24$, $p = .01$); however, adding these variables did not lead to a significant change in the proportion of explained variance ($\Delta R^2 = 0.05$, $\Delta F(3, 102) = 2.08$, $p = .11$), signifying that demographic variables alone explained a greater proportion of the variance in delayed memory than volume of the MTL white matter ROIs. Only age and sex were significantly related to delayed memory ($ß = -0.19$, $t(102) = -2.04$, $p = .04$ and $ß = 0.30$, $t(102) = 3.01$, $p = .003$, respectively). None of the white matter volumes reached significance; however, hippocampal cingulum volume exhibited a trending effect ($ß = -0.20$, $t(102) = -1.87$, $p = .06$).

In Step 3, adding CSF markers yielded a significant overall model ($R^2 = 0.17$, $F(8, 100) = 2.53$, $p = .02$), but once again, did not lead to a significant change in the proportion of explained variance ($\Delta R^2 = 0.01$, $\Delta F(2, 100) = 0.48$, $p = .62$). After accounting for the influence of CSF $A\beta_{42}$ and t-tau, sex remained significant ($ß = 0.32$, $t(100) = 3.12$, $p = .002$), but age did not ($ß = -0.17$, $t(100) = -1.84$, $p = .07$). No other variables reached significance, but hippocampal cingulum volume remained trending ($ß = -0.20$, $t(100) = -1.90$, $p = .06$).

Similar to the previous steps, in Step 4, the overall model was significant ($R^2 = 0.19$, $F(10, 98) = 2.29$, $p = .02$), but the addition of gray matter volumes did not result in a change in the overall proportion of explained variance ($\Delta R^2 = 0.02$, $\Delta F(2, 98) = 1.26$, $p = .29$). In this final step, age and sex were significant ($ß = -0.20$, $t(98) = -2.08$, $p = .04$ and $ß = 0.29$, $t(98) = 2.57$, $p = .01$, respectively), and volume of the UF was also found to uniquely contribute to the relationship with delayed memory performance ($ß = 0.26$, $t(98) = 2.18$, $p = .03$). Specifically, higher uncinate volume was related to better performance. No other variables reached significance (p's > .08).

4. Discussion

Despite the growing number of investigations of DTI and CSF markers, very few have examined the relative contributions of each type of measure to individual differences in cognition (for a review, see Alm and Bakker, 2019). In this study, we sought to investigate whether MRI and CSF measures, alone or in combination, provide a neurobiological basis for individual differences in episodic memory performance in a group of cognitively normal older adults. We utilized hierarchical linear regression analyses in order to tease apart the proportion of variance in episodic memory accounted for by each class of variables. Our findings demonstrate that DTI measures of MTL white matter tracts (specifically the fornix and hippocampal cingulum) account for a significant amount of the variance explained in a composite score of delayed episodic memory above and beyond demographic variables. Moreover, the DTI metrics for these ROIs were the only set of variables in the hierarchical regression model that significantly improved the proportion of explained variance, even with measures of AD CSF markers, gray matter volumes, and white matter volumes included in the models. This remained true even in models where the DTI variables were entered in the last step of the hierarchy, indicating that the findings were not merely an effect influenced by the order of variable entry into the models. This indicates that DTI microstructural metrics

for MTL regions exhibit a robust relationship with individual differences in episodic memory.

It should be noted that while RD measures yielded a significant increase in the variability explained by the overall regression model, the increase associated with MD metrics was only marginal ($p = .06$). However, the RD and MD models accounted for very similar proportions of explained variance (19% and 17% respectively), and the change in R^2 for MD measures surpassed the threshold for statistical significance in the model when MD values were entered last. Therefore, it seems that RD may be a slightly more robust measure in terms of relating brain structure to cognitive function. In line with this, RD is typically considered to be more sensitive to specific alterations in microstructure, as well as a more direct index of microstructure (Alexander et al., 2011).

Across the MD and RD indices, both the hippocampal cingulum and the fornix were uniquely associated with variability in delayed memory. Importantly, these associations were present across each of the steps within the hierarchical regression models, signifying robust relationships with episodic memory, above and beyond any effects of age, sex, education, CSF markers, and gray matter volumes. This suggests a strong association between individual differences in delayed memory and variability in the microstructure of hippocampal white matter tracts. Given that both pathways terminate in the hippocampus, this adds to the body of literature implicating the hippocampus in the facilitation of long term memory function (e.g. Nadel & Moscovitch, 1997; Squire & Alvarez, 1995; Squire, Genzel, Wixted, & Morris, 2015) by providing evidence that hippocampal white matter also seems to be critically involved in supporting episodic memory processes. Microstructural changes in the fornix and the hippocampal cingulum have also been previously reported across the stages of the AD continuum (Oishi et al., 2012; Zhang et al., 2007). Moreover, the associations with memory performance are consistent with prior studies relating microstructural variations to individual differences in episodic memory. Microstructure of the fornix and hippocampal cingulum have both demonstrated previous associations with memory performance in non-demented older adults (which may include individuals with MCI; Ezzati et al., 2016; Metzler-Baddeley et al., 2011a), as well as across the AD continuum (Lin et al., 2014; Mielke et al., 2012; Oishi et al., 2012).

Our findings extend the prior literature by demonstrating that these relationships for the fornix and hippocampal cingulum are present in a cohort of cognitively normal participants, even after accounting for potential contributions from CSF AD biomarkers and MTL gray matter volumes (adjusted for demographics). Furthermore, these brain-behavior associations were specific to fornix and hippocampal cingulum microstructure, since the same relationships did not emerge for the corresponding white matter volumes or the UF. Given that microstructural measures index the underlying properties of white matter tissue on a finer scale, it is possible that these metrics are better able to detect subtle alterations not present at the macrostructural level in cognitively normal individuals. Age-related microstructural changes in the UF may be more subtle and therefore not associated with episodic memory in cognitively normal individuals.

It is important to note the discrepancy in the directions of the hippocampal cingulum and fornix relationships with delayed memory. For the fornix, decreases in MD and RD were associated with better memory performance. In contrast, elevated MD and RD were both indicative of better performance for the hippocampal cingulum. However, this inconsistency was maintained in sensitivity analyses removing both 5% and 50% of cases, based on the Mahalanobis distance test for multivariate outliers (data not shown); therefore, it does not seem to merely be due to the influence of a few outliers. Additionally, the hippocampal cingulum relationships were not necessarily in the expected direction. MD is a measure of the average diffusion in a given voxel; thus, heightened MD values can indicate increased free diffusion, which is often interpreted as the presence of tissue damage (Soares et al., 2013). It was therefore surprising to find a positive relationship between hippocampal cingulum MD and delayed memory. Similarly, RD is a measurement that represents the degree of diffusion occurring perpendicular to the primary axis of diffusion, such that increases in RD tend to be associated with myelin loss (Alexander et al., 2011; Beaulieu, 2011; Jones et al., 2013; Tournier et al., 2011). However, these interpretations are based largely on animal studies and may not hold true for the much more complex connectome of the human brain. For instance, the assumption that fiber bundles run parallel to the primary axis of diffusion, and therefore increased diffusion in the perpendicular direction (i.e. RD) indicates some sort of damage does not always hold true for the human brain (Jones et al., 2013). An axon bundle consisting of fanning or crossing fibers will have varying diffusion orientations within the bundle. This could lead to a microstructure that appears to be less coherent and less anisotropic relative to a fiber bundle with the same number and quality of fibers, but containing axons all aligned in the same direction (Jones et al., 2013). Yet, this does not signify that one of the fiber bundles has higher “integrity” than the other, only that they differ in appearance. It is therefore critical to be particularly cautious when interpreting microstructural DTI effects.

With respect to the CSF biomarkers, the addition of $A\beta_{42}$ and t-tau to the hierarchical regression (and the ratio of t-tau/$A\beta_{42}$) did not improve the overall model. Furthermore, neither CSF marker was independently associated with delayed memory performance. This was not completely unexpected, however, since past examinations of cross-sectional relationships between CSF markers and episodic memory have yielded mixed results in cognitively normal cohorts. Some studies have reported significant cross-sectional associations (e.g. Pettigrew et al., 2015; Stomrud et al., 2010), while others have found no evidence of such relationships (e.g. Li et al., 2014; Rami et al., 2011; Rolstad et al., 2011; Schott et al., 2010; Vemuri et al., 2011); therefore, further research is needed on this topic. Of note, Pettigrew et al. (2015) reported an association between CSF t-tau and p-tau with visuospatial episodic memory, but not with verbal episodic memory as examined in the present study. It is possible, therefore, that measures of tau are more directly related to visuospatial episodic memory but not to measures of verbal episodic memory. It is also possible that alterations in CSF measurements (which reflect global rather than localized changes) are less likely to demonstrate associations with episodic memory performance among cognitively normal individuals.

Similar to the CSF markers, the inclusion of gray matter volumes corresponding to the entorhinal area and hippocampus did not change the amount of variance accounted for by

the overall model. Additionally, neither entorhinal volume nor hippocampal volume demonstrated a significant relationship with memory performance. This was surprising, given both regions' importance in episodic memory function, and the significance of the entorhinal cortex as one of the earliest regions to undergo pathological changes in AD (Braak and Braak, 1991). It is possible that macrostructural measures of these brain regions are significant predictors of progression to MCI, but are not strongly associated with cross-sectional differences in cognition among cognitively normal individuals. It is also possible that more subtle shape-based gray matter measures of the hippocampus or entorhinal cortex may be more sensitive to individual differences in episodic memory among cognitively normal individuals (e.g. Miller et al., 2013).

Finally, in a hierarchical model with MTL white matter volumes as the independent measures of interest, the addition of the other variables described above did not improve the overall model. In general, this again suggests that detecting effects in a cognitively normal cohort may necessitate a more sensitive measure than volume; however, there was one particular white matter volume ROI that did yield a significant effect. Greater UF volume was associated with better delayed memory performance, but only in the final step. This finding requires further replication.

4.1. Limitations and Future Directions

The primary limitation of the present study is the cross-sectional nature of the investigation. Future studies will be able to take advantage of the longitudinal data currently being collected, which can examine not only the relationship between white matter microstructure and episodic memory, but also how the relationship may change over time. Longitudinal assessments will also aid in disentangling whether DTI measures are predictive of clinical decline or whether they may reflect age-related changes that are independent of AD.

Several technical issues are also potential limitations. One concerns conclusions drawn from correlations between DTI indices and behavior. As discussed above, much is still unknown with respect to interpreting directionality of brain-behavior relationships in the context of DTI microstructure. Thicker myelination in general may not always lead to enhanced performance on a cognitive task (Scholz et al., 2009). Although myelination is typically thought to enhance signal transduction, improved neural efficiency may also be achieved through mechanisms like synaptic pruning, which could yield local decreases in myelination. Microstructural findings are also vulnerable to overinterpretations about the overall integrity of structural connections throughout the brain. DTI metrics are derived on a voxel by voxel basis; thus, conclusions drawn from such local changes may not be generalizable to the human connectome on a broader scale. We must therefore be wary not to over-attribute changes in local microstructure to alterations in more global integrity of white matter.

Additionally, it should be noted that ROI-based analyses of small fiber pathways, such as the fornix, are particularly prone to partial volume effects that occur from signal contamination due to the close proximity of CSF (Metzler-Baddeley et al., 2011b; Vos et al., 2011). Although this is more of a concern in samples with known atrophy, since volume reductions can exacerbate partial volume effects (Oishi and Lyketsos, 2014), we still sought to mitigate

this issue. We conducted a follow-up analysis controlling for the volumes of the white matter ROIs, and our pattern of results was unchanged. Therefore, it does not seem that our findings were solely due to the influence of partial volume effects; however, we still caution against overinterpretation of the anatomical changes that may be represented by changes in diffusivity. Future studies would benefit from utilization of recent advances in DTI sequence development that can facilitate the reduction of partial volume effects and improve the ability to distinguish particular pathways, such as multi-shell acquisitions with higher b-values.

It is also possible that variation in gray matter volumes may contribute to the relationships found between episodic memory and white matter microstructure. Volume differences in the gray matter regions from which the white matter pathways emanate may be driving the DTI effects. However, the effects in the hippocampal cingulum and fornix remained significant even after controlling for the potential influence of gray matter volume differences across participants, suggesting that our findings cannot solely be explained by volume differences.

4.2. Conclusions

Very few studies have directly compared the relative contributions of DTI and CSF markers to individual differences in cognition. The hierarchical regression analyses used in the present study allowed us to assess the unique contribution of each class of variables to variability in episodic memory. Our findings suggest that DTI metrics can provide indices of the underlying microstructure of white matter pathways in the medial temporal lobe that are sensitive enough to capture individual differences in episodic memory performance among cognitively normal individuals. These subtle microstructural alterations exhibited robust associations with delayed episodic memory, suggesting that they may be useful in identifying changes associated with the initial phases of AD.

It is possible that the relationships exhibited between DTI metrics and individual differences in memory function could be used to improve the selection of clinical trial candidates, as well as provide critical co-variates in the analysis of outcome measures. These relationships could also be used to track subject-specific trajectories of disease progression.

Supplementary Material

Refer to Web version on PubMed Central for supplementary material.

Acknowledgements

This work was supported in part by grants from the National Institutes of Health (U19-AG033655, P50-AG005146, and T32-AG027668). We thank the entire BIOCARD study team at Johns Hopkins University for their support, the BIOCARD participants for continuing to participate in the study, and the Geriatric Psychiatry Branch of the intramural program of the NIMH who initiated this study (PI: Dr. Trey Sunderland).

References

Acosta-Cabronero J, Williams GB, Pengas G, Nestor PJ, 2010 Absolute diffusivities define the landscape of white matter degeneration in Alzheimer’s disease. Brain 133, 529–539. 10.1093/brain/awp257 [PubMed: 19914928]

Albert MS, DeKosky ST, Dickson D, Dubois B, Feldman HH, Fox NC, Gamst A, Holtzman DM, Jagust WJ, Petersen RC, Snyder PJ, Carrillo MC, Thies B, Phelps CH, 2011 The diagnosis of mild cognitive impairment due to Alzheimer's disease: Recommendations from the National Institute on Aging-Alzheimer's Association workgroups on diagnostic guidelines for Alzheimer's disease. Alzheimer's Dement. 7, 270–279. 10.1016/j.jalz.2011.03.008 [PubMed: 21514249]

Albert MS, Soldan A, Gottesman R, McKhann G, Sacktor N, Farrington L, Grega M, Turner R, Lu Y, Li S, Wang M-C, Selnes O, 2014 Cognitive changes preceding clinical symptom onset of mild cognitive impairment and relationship to ApoE genotype. Curr. Alzheimer Res 11, 773–84. 10.2174/1567205011081409101219 20 [PubMed: 25212916]

Alexander AL, Hurley SA, Samsonov AA, Adluru N, Hosseinbor AP, Mossahebi P, Tromp DPM, Zakszewski E, Field AS, 2011 Characterization of cerebral white matter properties using quantitative magnetic resonance imaging stains. Brain Connect. 1, 423–446. 10.1089/brain.2011.0071 [PubMed: 22432902]

Alm KH, Bakker A, 2019 Relationships between diffusion tensor imaging and cerebrospinal fluid metrics in early stages of the Alzheimer's disease continuum. J. Alzheimer's Dis 70, 965–981. 10.3233/jad-181210 [PubMed: 31306117]

Alzheimer's Association, 2017 2017 Alzheimer's disease facts and figures. Alzheimers Dement. 13, 325–373. 10.1016/j.jalz.2017.02.001

Amlien IK, Fjell AM, 2014 Diffusion tensor imaging of white matter degeneration in Alzheimer's disease and mild cognitive impairment. Neuroscience 276, 206–215. 10.1016/j.neuroscience.2014.02.017 [PubMed: 24583036]

Beaulieu C, 2011 What makes diffusion anisotropic in the nervous system, in: Jones DK (Ed.), Diffusion MRI: Theory, Methods, and Applications. Oxford University Press, New York, pp. 92–109.

Bennett IJ, Madden DJ, 2014 Disconnected aging: Cerebral white matter integrity and age-related differences in cognition. Neuroscience 276, 187–205. 10.1016/j.neuroscience.2013.11.026 [PubMed: 24280637]

Braak H, Braak E, 1991 Neuropathological stageing of Alzheimer-related changes. Acta Neuropathol. 82, 239–259. 10.1007/BF00308809 [PubMed: 1759558]

Caso F, Agosta F, Filippi M, 2016 Insights into white matter damage in Alzheimer's disease: From postmortem to in vivo diffusion tensor MRI studies. Neurodegener. Dis 16, 26–33. 10.1159/000441422 [PubMed: 26618812]

Ceritoglu C, Oishi K, Li X, Chou MC, Younes L, Albert M, Lyketsos C, van Zijl PCM, Miller MI, Mori S, 2009 Multi-contrast large deformation diffeomorphic metric mapping for diffusion tensor imaging. Neuroimage 47, 618–627. 10.1016/j.neuroimage.2009.04.057 [PubMed: 19398016]

Christensen GE, Joshi SC, Miller MI, 1997 Volumetric transformation of brain anatomy. IEEE Trans. Med. Imaging 16, 864–877. 10.1109/42.650882 [PubMed: 9533586]

Clerx L, Visser PJ, Verhey F, Aalten P, 2012 New MRI markers for Alzheimer's disease: A meta-analysis of diffusion tensor imaging and a comparison with medial temporal lobe measurements. J. Alzheimer's Dis 29, 405–429. 10.3233/JAD-2011-110797 [PubMed: 22330833]

Contreras JA, Goñi J, Risacher SL, Sporns O, Saykin AJ, 2015 The Structural and Functional Connectome and Prediction of Risk for Cognitive Impairment in Older Adults. Curr. Behav. Neurosci. Reports 2, 234–245. 10.1007/s40473-015-0056-z

Ezzati A, Katz MJ, Lipton ML, Zimmerman ME, Lipton RB, 2016 Hippocampal volume and cingulum bundle fractional anisotropy are independently associated with verbal memory in older adults. Brain Imaging Behav. 10, 652–659. 10.1007/s11682-015-9452-y [PubMed: 26424564]

Fagan AM, Roe CM, Xiong C, Mintun MA, Morris JC, Holtzman DM, 2007 Cerebrospinal fluid tau/beta-amyloid42 ratio as a prediction of cognitive decline in nondemented older adults. Arch. Neurol 64, 343–349. [PubMed: 17210801]

Gold BT, Johnson NF, Powell DK, Smith CD, 2012 White matter integrity and vulnerability to Alzheimer's disease: Preliminary findings and future directions. Biochim. Biophys. Acta 1822, 416–422. 10.1016/j.bbadis.2011.07.009 [PubMed: 21803153]

Grenander U, Miller MI, 1998 Computational anatomy: An emerging discipline. Q. Appl. Math 56, 617–694.

Gustafson DR, Skoog I, Rosengren L, Zetterberg H, Blennow K, 2007 Cerebrospinal fluid β-amyloid 1–42 concentration may predict cognitive decline in older women. J. Neurol. Neurosurg. Psychiatry 78, 461–464. 10.1136/jnnp.2006.100529 [PubMed: 17098843]

Hiyoshi-Taniguchi K, Oishi N, Namiki C, Miyata J, Murai T, Cichocki A, Fukuyama H, 2015 The uncinate fasciculus as a predictor of conversion from aMCI to Alzheimer disease. J. Neuroimaging 25, 748–753. 10.1111/jon.12196 [PubMed: 25491469]

Jiang H, Van Zijl PCM, Kim J, Pearlson GD, Mori S, 2006 DtiStudio: Resource program for diffusion tensor computation and fiber bundle tracking. Comput. Methods Programs Biomed 81, 106–116. 10.1016/j.cmpb.2005.08.004 [PubMed: 16413083]

Jones DK, Knösche TR, Turner R, 2013 White matter integrity, fiber count, and other fallacies: The do's and don'ts of diffusion MRI. Neuroimage 73, 239–254. 10.1016/j.neuroimage.2012.06.081 [PubMed: 22846632]

Lam CLM, Yiend J, Lee TMC, 2017 Imaging and neuropsychological correlates of white matter lesions in different subtypes of Mild Cognitive Impairment: A systematic review. NeuroRehabilitation 41, 189–204. 10.3233/NRE-171471 [PubMed: 28527230]

Leow AD, Zhan L, Zhu S, Hageman N, Barysheva M, Toga AW, McMahon KL, de Zubicaray GI, Wright MJ, Thompson PM, 2009 White matter integrity measured by fractional anisotropy correlates poorly with actual individual fiber anisotropy. 2009 IEEE Int. Symp. Biomed. Imaging From Nano to Macro 622–625. 10.1109/ISBI.2009.5193124

Li G, Millard SP, Peskind ER, Zhang J, Yu CE, Leverenz JB, Mayer C, Shofer JS, Raskind MA, Quinn JF, Galasko DR, Montine TJ, 2014 Cross-sectional and longitudinal relationships between cerebrospinal fluid biomarkers and cognitive function in people without cognitive impairment from across the adult life span. JAMA Neurol. 71, 742–751. 10.1001/jamaneurol.2014.445 [PubMed: 24756381]

Lin Y-C, Shih Y-C, Tseng W-YI, Chu Y-H, Wu M-T, Chen T-F, Tang P-F, Chiu M-J, 2014 Cingulum correlates of cognitive functions in patients with mild cognitive impairment and early Alzheimer's disease: A diffusion spectrum imaging study. Brain Topogr. 27, 393–402. 10.1007/s10548-013-0346-2 [PubMed: 24414091]

McKhann GM, Knopman DS, Chertkow H, Hyman BT, Jack CR, Kawas CH, Klunk WE, Koroshetz WJ, Manly JJ, Mayeux R, Mohs RC, Morris JC, Rossor MN, Scheltens P, Carrillo MC, Thies B, Weintraub S, Phelps CH, 2011 The diagnosis of dementia due to Alzheimer's disease: Recommendations from the National Institute on Aging-Alzheimer's Association workgroups on diagnostic guidelines for Alzheimer's disease. Alzheimer's Dement. 7, 263–269. 10.1016/j.jalz.2011.03.005 [PubMed: 21514250]

Metzler-Baddeley C, Jones DK, Belaroussi B, Aggleton JP, O'Sullivan MJ, 2011a Frontotemporal connections in episodic memory and aging: A diffusion MRI tractography study. J. Neurosci 31, 13236–13245. [PubMed: 21917806]

Metzler-Baddeley C, Jones DK, Pasternak O, Bells S, O'Sullivan MJ, 2011b How and how not to correct for CSF-contamination in diffusion MRI. Neuroimage 59, 1394–1403. 10.1016/j.neuroimage.2011.08.043 [PubMed: 21924365]

Mielke MM, Okonkwo OC, Oishi K, Mori S, Tighe S, Miller MI, Ceritoglu C, Brown T, Albert M, Lyketsos CG, 2012 Fornix integrity and hippocampal volume predict memory decline and progression to Alzheimer's disease. Alzheimer's Dement. 8, 105–113. 10.1016/j.jalz.2011.05.2416 [PubMed: 22404852]

Miller M, Banerjee A, Christensen G, Joshi S, Khaneja N, Grenander U, Matejic L, 1997 Statistical methods in computational anatomy. Stat. Methods Med. Res 6, 267–299. 10.1191/096228097673360480 [PubMed: 9339500]

Miller MI, Ratnanather JT, Tward DJ, Brown T, Lee DS, Ketcha M, Mori K, Wang M-C, Mori S, Albert MS, Younes L, 2015a Network Neurodegeneration in Alzheimer's Disease via MRI Based Shape Diffeomorphometry and High-Field Atlasing. Front. Bioeng. Biotechnol. 3, 1–16. 10.3389/fbioe.2015.00054

Miller MI, Younes L, Ratnanather JT, Brown T, Trinh H, Lee DS, Tward D, Mahon PB, Mori S, Albert M, 2015b Amygdalar atrophy in symptomatic Alzheimer's disease based on diffeomorphometry: The BIOCARD cohort. Neurobiol. Aging 36, S3–S10. 10.1016/j.neurobiolaging.2014.06.032 [PubMed: 25444602]

Miller MI, Younes L, Ratnanather JT, Brown T, Trinh H, Postell E, Lee DS, Wang MC, Mori S, O'Brien R, Albert M, 2013 The diffeomorphometry of temporal lobe structures in preclinical Alzheimer's disease. NeuroImage Clin. 3, 352–360. 10.1016/j.nicl.2013.09.001 [PubMed: 24363990]

Moghekar A, Li S, Lu Y, Li M, Wang MC, Albert M, O'Brien R, 2013 CSF biomarker changes precede symptom onset of mild cognitive impairment. Neurology 81, 1753–1758. 10.1212/01.wnl.0000435558.98447.17 [PubMed: 24132375]

Mori S, Wu D, Li Y, Kolasny A, Vaillant MA, Faria AV, Oishi K, Miller MI, 2016 MRICloud: Delivering high-throughput MRI neuroinformatics as cloud-based software as a service. Comput. Sci. Eng 18, 21–35.

Nadel L, Moscovitch M, 1997 Memory consolidation and the hippocampal complex. Curr. Opin. Neurobiol 7, 217–227. 10.1016/S0959-4388(97)80010-4 [PubMed: 9142752]

Nobili F, Arnaldi D, Roccatagliata L, Chincarini A, Accardo J, Picco A, Ferrara M, Buschiazzo A, Morbelli S, 2014 Neuroimaging findings in mild cognitive impairment, in: Dierckx RAJO, Leenders KL, De Vries EFJ, Van Waarde A (Eds.), Pet and Spect in Neurology. pp. 271–306. 10.1007/978-3-642-54307-4

Oishi K, Lyketsos CG, 2014 Alzheimer's disease and the fornix. Front. Aging Neurosci 6, 1–9. 10.3389/fnagi.2014.00241 [PubMed: 24478697]

Oishi K, Mielke MM, Albert M, Lyketsos CG, 2011 DTI analyses and clinical applications in Alzheimer's disease. J. Alzheimer's Dis 26, 287–296. 10.3233/JAD-2011-0007 [PubMed: 21971468]

Oishi K, Mielke MM, Albert M, Lyketsos CG, Mori S, 2012 The fornix sign: A potential sign for alzheimer's disease based on diffusion tensor imaging. J. Neuroimaging 22, 365–374. 10.1111/j.1552-6569.2011.00633.x [PubMed: 21848679]

Pettigrew C, Soldan A, Moghekar A, Wang MC, Gross AL, O'Brien R, Albert M, 2015 Relationship between cerebrospinal fluid biomarkers of Alzheimer's disease and cognition in cognitively normal older adults. Neuropsychologia 78, 63–72. 10.1016/j.neuropsychologia.2015.09.024 [PubMed: 26394023]

Radanovic M, Pereira FRSR, Stella F, Aprahamian I, Ferreira LKK, Forlenza OVV, Busatto GF, 2013 White matter abnormalities associated with Alzheimer's disease and mild cognitive impairment: A critical review of MRI studies. Expert Rev. Neurother 13, 483–493. 10.1586/ern.13.45 [PubMed: 23621306]

Rami L, Fortea J, Bosch B, Solé-Padullés C, Lladó A, Iranzo A, Sánchez-Valle R, Molinuevo JL, 2011 Cerebrospinal fluid biomarkers and memory present distinct associations along the continuum from healthy subjects to AD patients. J. Alzheimer's Dis 23, 319–326. 10.3233/JAD-2010-101422 [PubMed: 21098971]

Rolstad S, Berg AI, Bjerke M, Blennow K, Johansson B, Zetterberg H, Wallin A, 2011 Amyloid-β42 is associated with cognitive impairment in healthy elderly and subjective cognitive impairment. J. Alzheimer's Dis 26, 135–142. 10.3233/JAD-2011-110038

Scholz J, Tomassini V, Johansen-Berg H, 2009 Individual differences in white matter microstructure in the healthy brain, in: Johansen-Berg H, Behrens TEJ (Eds.), Diffusion MRI: From Quantitative Measurement to In Vivo Neuroanatomy. Elsevier Inc, London, UK, pp. 237–249. 10.1016/B978-0-12-396460-1.00014-7

Schott JM, Bartlett JW, Fox NC, Barnes J, 2010 Increased brain atrophy rates in cognitively normal older adults with low cerebrospinal fluid Aβ1–42. Ann. Neurol 68, 825–834. 10.1002/ana.22315 [PubMed: 21181717]

Soares JM, Marques P, Alves V, Sousa N, 2013 A hitchhiker's guide to diffusion tensor imaging. Front. Neurosci 7, 1–14. 10.3389/fnins.2013.00031 [PubMed: 23386807]

Soldan A, Pettigrew C, Cai Q, Wang MC, Moghekar AR, O'Brien RJ, Selnes OA, Albert MS, Rodzon B, Gottesman R, Sacktor N, McKhann G, Turner S, Farrington L, Grega M, Rudow G, D'Agostino D, Rudow S, Miller M, Mori S, Ratnanather T, Brown T, Chi H, Kolasny A, Oishi K, Reigel T, Younes L, Spangler A, Scherer R, Shade D, Ervin A, Jones J, Toepfner M, Parlett L, Patterson A, Mohammed A, Lu D, Troncoso J, Crain B, Pletnikova O, Fisher K, 2016 Hypothetical preclinical Alzheimer disease groups and longitudinal cognitive change. JAMA Neurol. 73, 698–705. 10.1001/jamaneurol.2016.0194 [PubMed: 27064267]

Soldan A, Pettigrew C, Lu Y, Wang M-C, Selnes O, Albert M, Brown T, Ratnanather JT, Younes L, Miller MI, 2015 Relationship of medial temporal lobe atrophy, APOE genotype, and cognitive reserve in preclinical Alzheimer's disease. Hum. Brain Mapp 36, 2826–2841. 10.1002/hbm.22810 [PubMed: 25879865]

Sperling RA, Aisen PS, Beckett LA, Bennett DA, Craft S, Fagan AM, Iwatsubo T, Jack CR, Kaye J, Montine TJ, Park DC, Reiman EM, Rowe CC, Siemers E, Stern Y, Yaffe K, Carrillo MC, Thies B, Morrison-Bogorad M, Wagster MV, Phelps CH, 2011 Toward defining the preclinical stages of Alzheimer's disease: Recommendations from the National Institute on Aging-Alzheimer's Association workgroups on diagnostic guidelines for Alzheimer's disease. Alzheimer's Dement. 7, 280–292. 10.1016/j.jalz.2011.03.003 [PubMed: 21514248]

Squire LR, Alvarez P, 1995 Retrograde amnesia and memory consolidation: A neurobiological perspective. Curr. Opin. Neurobiol 5, 169–177. [PubMed: 7620304]

Squire LR, Genzel L, Wixted JT, Morris RG, 2015 Memory Consolidation. Cold Spring Harb. Perspect. Biol 7, 1–21.

Stomrud E, Hansson O, Zetterberg H, Blennow K, Minthon L, Londos E, 2010 Correlation of longitudinal cerebrospinal fluid biomarkers with cognitive decline in healthy older adults. Arch. Neurol 67, 217–223. 10.1001/archneurol.2009.316 [PubMed: 20142530]

Tang X, Yoshida S, Hsu J, Huisman TAGM, Faria AV, Oishi K, Kutten K, Poretti A, Li Y, Miller MI, Mori S, 2014 Multi-contrast multi-atlas parcellation of diffusion tensor imaging of the human brain. PLoS One 9, e96985 10.1371/journal.pone.0096985 [PubMed: 24809486]

Teipel SJ, Grothe MJ, Zhou J, Sepulcre J, Dyrba M, Sorg C, Babiloni C, 2016 Measuring cortical connectivity in Alzheimer's disease as a brain neural network pathology: Toward clinical applications. J. Int. Neuropsychol. Soc 22, 138–163. 10.1017/S1355617715000995 [PubMed: 26888613]

Thal DR, Rüb U, Orantes M, Braak H, 2002 Phases of A beta-deposition in the human brain and its relevance for the development of AD. Neurology 58, 1791–800. 10.1212/WNL.58.12.1791 [PubMed: 12084879]

Tournier J-D, Mori S, Leemans A, 2011 Diffusion tensor imaging and beyond. Magn. Reson. Med 65, 1532–1556. 10.1002/mrm.22924 [PubMed: 21469191]

Vemuri P, Weigand SD, Przybelski SA, Knopman DS, Smith GE, Trojanowski JQ, Shaw LM, Decarli CS, Carmichael O, Bernstein MA, Aisen PS, Weiner M, Petersen RC, Jack CR, 2011 Cognitive reserve and Alzheimer's disease biomarkers are independent determinants of cognition. Brain 134, 1479–1492. 10.1093/brain/awr049 [PubMed: 21478184]

Vos SB, Jones DK, Viergever MA, Leemans A, 2011 Partial volume effect as a hidden covariate in DTI analyses. Neuroimage 55, 1566–1576. 10.1016/j.neuroimage.2011.01.048 [PubMed: 21262366]

Vos SJ, Xiong C, Visser PJ, Jasielec MS, Hassenstab J, Grant EA, Cairns NJ, Morris JC, Holtzman DM, Fagan AM, 2013 Preclinical Alzheimer's disease and its outcome: a longitudinal cohort study. Lancet Neurol. 12, 957–965. 10.1016/S1474-4422(13)70194-7 [PubMed: 24012374]

Zhang B, Xu Y, Zhu B, Kantarci K, 2014 The role of diffusion tensor imaging in detecting microstructural changes in prodromal Alzheimer's disease. CNS Neurosci. Ther 20, 3–9. 10.1111/cns.12166 [PubMed: 24330534]

Zhang Y, Schuff N, Jahng G-H, Bayne W, Mori S, Schad L, Mueller S, Du A-T, Kramer JH, Yaffe K, Chui H, Jagust WJ, Miller BL, Weiner MW, 2007 Diffusion tensor imaging of cingulum fibers in mild cognitive impairment and Alzheimer disease. Neurology 68, 13–19. 10.1212/01.wnl.0000250326.77323.01 [PubMed: 17200485]

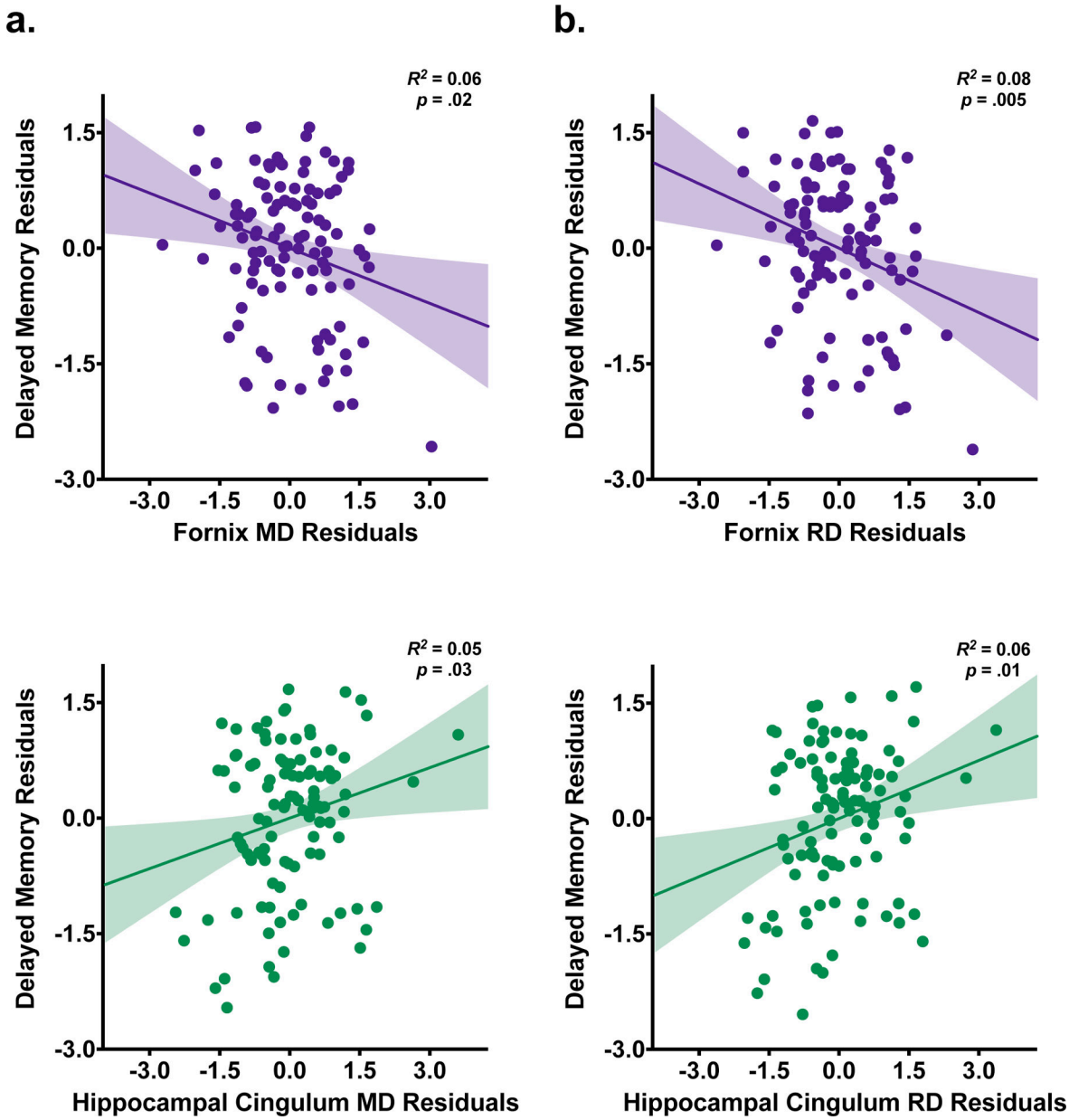

Figure 1. Delayed memory performance associations with white matter microstructure.
Partial regression plots with standardized residuals depicting the relationship of delayed episodic memory performance with fornix and hippocampal cingulum microstructure from the final step of the hierarchical regression model using mean diffusivity (MD) as the primary DTI metric of interest (a) and the final step of the hierarchical regression model using radial diffusivity (RD) as the primary DTI metric of interest (b).

Table 1.

Mean MTL MD explaining variability in delayed episodic memory composite (N = 109)

Delayed memory composite score	Independent variables	ß	*t*-value	*F*	Δ*F*	R^2	ΔR^2
Step 1				**4.27****		0.11	
	Age	−0.17	−1.85†				
	Sex	0.26	**2.79****				
	Education	−0.06	−0.62				
Step 2				**3.53****	2.60†	0.17	0.06
	Age	−0.02	−0.17				
	Sex	0.28	**3.05****				
	Education	−0.05	−0.58				
	Hippocampal Cingulum MD	0.26	**2.38***				
	Fornix MD	−0.29	**−2.18***				
	Uncinate MD	−0.05	−0.45				
Step 3				**2.74****	0.46	0.18	0.01
	Age	0.01	0.10				
	Sex	0.29	**3.13****				
	Education	−0.06	−0.59				
	Hippocampal Cingulum MD	0.26	**2.32***				
	Fornix MD	−0.31	**−2.29***				
	Uncinate MD	−0.06	−0.51				
	$A\beta_{42}$	−0.01	−0.08				
	t-tau	−0.09	−0.89				
Step 4				**2.33***	0.77	0.19	0.01
	Age	0.01	0.05				
	Sex	0.27	**2.47***				
	Education	−0.05	−0.55				
	Hippocampal Cingulum MD	0.25	**2.22***				
	Fornix MD	−0.34	**−2.43***				
	Uncinate MD	−0.06	−0.50				
	$A\beta_{42}$	−0.01	−0.12				
	t-tau	−0.09	−0.91				
	Entorhinal volume	−0.10	−0.94				
	Hippocampal volume	−0.07	−0.62				

$^{\dagger}p < .07$;

$^{*}p < .05$;

$^{**}p < .01$;

MD: mean diffusivity; MTL: medial temporal lobe

Table 2.

Mean MTL RD explaining variability in delayed episodic memory composite (N = 109)

Delayed memory composite score	Independent variables	ß	*t*-value	*F*	Δ*F*	R^2	ΔR^2
Step 1				**4.27** **		0.11	
	Age	−0.17	−1.85 †				
	Sex	0.26	**2.79** **				
	Education	−0.06	−0.62				
Step 2				**4.03** ***	**3.48** *	0.19	0.08
	Age	−0.03	−0.21				
	Sex	0.27	**2.99** **				
	Education	−0.06	−0.62				
	Hippocampal Cingulum RD	0.31	**2.71** **				
	Fornix RD	−0.37	**–2.65** **				
	Uncinate RD	0.02	0.16				
Step 3				**3.16** **	0.62	0.20	0.01
	Age	0.02	0.13				
	Sex	0.29	**3.10** **				
	Education	−0.06	−0.63				
	Hippocampal Cingulum RD	0.31	**2.72** **				
	Fornix RD	−0.40	**–2.80** **				
	Uncinate RD	0.01	0.07				
	$A\beta_{42}$	−0.01	−0.11				
	t-tau	−0.10	−1.03				
Step 4				**2.63** **	0.61	0.21	0.01
	Age	0.01	0.10				
	Sex	0.26	**2.43** *				
	Education	−0.06	−0.60				
	Hippocampal Cingulum RD	0.30	**2.58** **				
	Fornix RD	−0.43	**–2.88** **				
	Uncinate RD	0.002	0.02				
	$A\beta_{42}$	−0.02	−0.16				
	t-tau	−0.11	−1.06				
	Entorhinal volume	−0.08	−0.80				
	Hippocampal volume	−0.06	−0.60				

$^{\dagger}p < .07$;

$^{*}p < .05$;

$^{**}p < .01$;

$^{***}p < .001$;

RD: radial diffusivity; MTL: medial temporal lobe

Table 3.

Mean MTL white matter volumes explaining variability in delayed episodic memory composite (N = 109)

Delayed memory composite score	Independent variables	ß	*t*-value	*F*	Δ*F*	R^2	ΔR^2
Step 1				**4.27** **		0.11	
	Age	−0.17	−1.85 †				
	Sex	0.26	**2.79** **				
	Education	−0.06	−0.62				
Step 2							
	Age	−0.19	**−2.04** *	**3.24** **	2.08	0.16	0.05
	Sex	0.30	**3.01** **				
	Education	−0.05	−0.55				
	Hippocampal Cingulum volume	−0.20	−1.87 †				
	Fornix volume	0.12	1.30				
	Uncinate volume	0.19	1.69				
Step 3				**2.53** *	0.48	0.17	0.01
	Age	−0.17	−1.84 †				
	Sex	0.32	**3.12** **				
	Education	−0.06	−0.63				
	Hippocampal Cingulum volume	−0.20	−1.90 †				
	Fornix volume	0.13	1.37				
	Uncinate volume	0.19	1.72				
	$A\beta_{42}$	−0.03	−0.33				
	t-tau	−0.08	−0.79				
Step 4				**2.29** *	1.26	0.19	0.02
	Age	−0.20	**−2.08** *				
	Sex	0.29	**2.57** **				
	Education	−0.06	−0.60				
	Hippocampal Cingulum volume	−0.19	−1.76				
	Fornix volume	0.14	1.50				
	Uncinate volume	0.26	**2.18** *				
	$A\beta_{42}$	−0.04	−0.36				
	t-tau	−0.08	−0.85				
	Entorhinal volume	−0.09	−0.90				
	Hippocampal volume	−0.15	−1.28				

† $p < .07$;

* $p < .05$;

** $p < .01$;

MTL: medial temporal lobe